Published online 3 April 2017

Nucleic Acids Research, 2017, Vol. 45, No. 9 ***5309–5322***
doi: 10.1093/nar/gkx231

Intra-endosomal trafficking mediated by lysobisphosphatidic acid contributes to intracellular release of phosphorothioate-modified antisense oligonucleotides

Shiyu Wang[1,*], Hong Sun[1], Michael Tanowitz[2], Xue-hai Liang[1] and Stanley T. Crooke[1]

[1]Department of Core Antisense Research, Ionis Pharmaceuticals, Inc. 2855 Gazelle Court, Carlsbad, CA 92010, USA and [2]Department of Medicinal Chemistry, Ionis Pharmaceuticals, Inc. 2855 Gazelle Court, Carlsbad, CA 92010, USA

Received January 31, 2017; Revised March 22, 2017; Editorial Decision March 23, 2017; Accepted March 27, 2017

ABSTRACT

Antisense oligonucleotides (ASOs) with phosphorothioate (PS) linkages are broadly used as research tools and therapeutic agents. Chemically modified PS-ASOs can mediate efficient target reduction by site-specific cleavage of RNA through RNase H1. PS-ASOs are known to be internalized via a number of endocytotic pathways and are released from membrane-enclosed endocytotic organelles, mainly late endosomes (LEs). This study was focused on the details of PS-ASO trafficking through endocytic pathways. It was found that lysobisphosphatidic acid (LBPA) is required for release of PS-ASOs from LEs. PS-ASOs exited early endosomes (EEs) rapidly after internalization and became co-localized with LBPA by 2 hours in LEs. Inside LEs, PS-ASOs and LBPA were co-localized in punctate, dot-like structures, likely intraluminal vesicles (ILVs). Deactivation of LBPA using anti-LBPA antibody significantly decreased PS-ASO activities without affecting total PS-ASO uptake. Reduction of Alix also substantially decreased PS-ASO activities without affecting total PS-ASO uptake. Furthermore, Alix reduction decreased LBPA levels and limited co-localization of LBPA with PS-ASOs at ILVs inside LEs. Thus, the fusion properties of ILVs, which are supported by LBPA, contribute to PS-ASO intracellular release from LEs.

INTRODUCTION

Antisense oligonucleotides (ASOs) are widely used as research tools and therapeutic agents (1). ASOs can direct sequence-specific cleavage of target RNAs by a conserved mechanism mediated by endonuclease RNase H1 (2). To improve chemical stability and pharmacological efficacy, ASOs are generally linked via phosphorothioate (PS) backbone and terminal residues are modified with 2′-*O*-methoxyethyl (MOE) at the 2′-position of the ribose (3). PS-ASOs are effective even when they are applied to cells without prior complexation in liposomes or conjugation to cell-penetrating peptides (4). Although molecular details of the process of endocytic internalization of PS-ASOs may depend on the type of cell, PS-ASOs are able to escape from intracellular organelles in endocytotic pathways (5,6). Understanding the mechanisms by which PS-ASOs release from those membrane enclosed organelles is critical to understand the processes of uptake that lead to accumulation of PS-ASO at target sites (productive uptake).

Recently, it was found that intracellular trafficking plays an important role in regulating the pharmacological activity of PS-ASOs (7). It was proposed that there are productive and less-productive cellular uptake or distribution routes of PS-ASOs (7). Substances, such as PS-ASOs, endocytosed by different pathways are generally delivered to early endosomes (EEs) (8,9). EEs determine whether molecules are routed back to the cell surface through recycling endosomes or into late endosomes (LEs), also called multivesicular bodies (MVBs) (9). Cargos in LEs are packaged for degradation through 'non-productive' pathways such as lysosomes, for exosome secretion upon fusion with plasma membranes, or for being released intracellularly through back fusion processes (9). PS-ASOs were shown to traffic rapidly through EEs, resulting in progressive increases of target cleavage, suggesting that productive PS-ASO release mainly occurs at LEs (8). Thus, a small portion released from LEs/MVBs appears to be productive; while the larger portion remained in LE/lysosomes is non-productive. It is still not known how PS-ASO intracellular release processes are modulated by membrane fusion events at LEs.

One of intrinsic features of the endosomal pathway from EEs to LEs is the biogenesis of intralumenal vesicles (ILVs).

*To whom correspondence should be addressed. Tel: +1 760 603 2363; Fax: +1 760 603 2600; Email: swang@ionisph.com

There are two major mechanisms involved in ILV formation. One involves the protein machinery that recognizes ubiquitin to assemble the endosomal sorting complexes required for transport (ESCRT) proteins; the ESCRT proteins potentiate ILV formation beginning in EEs (10,11). The other mechanism is lipid mediated, mainly by bis(monoacylglycero)phosphate/lysobisphosphatidic acid (BMP/LBPA) (12,13). ILV formation is mechanistically coupled with membrane invagination or budding (14). LBPA is uniquely present at LEs and indispensable for LE membrane deformation (13). ILVs can fuse back to LE membranes to exchange lipid or protein contents. The release of cargo into the cytosol through this process is referred to as back fusion (15). It is not known whether PS-ASOs can be sorted to ILVs and which mechanisms contribute to the formation of such ILVs. Nor is it known whether back fusion processes are one of the productive pathways resulting in the release of PS-ASOs from LEs.

Here, we sought to determine the mechanism through which PS-ASOs are productively released from LEs. We first determined that the pharmacological activities of PS-ASOs require intracellular release from endocytic pathways. We then focused on the details of PS-ASOs trafficking through endocytic pathways. We found that PS-ASOs exit EEs rapidly after internalization and become co-localized with LBPA within 2 h. The co-localization between PS-ASOs and LBPA was also observed inside LEs. The presence of PS-ASOs at ILVs was confirmed in cells overexpressing a constitutively active form of Rab5(Q79L). To determine how the formation of ILVs contributes to productive ASO release, we first reduced the key components of ESCRT complexes, HRS and TSG101, and found that these proteins do not regulate PS-ASO activity. We further demonstrated a positive regulatory role of LBPA in PS-ASO release using an antibody that deactivates LBPA, or by reducing Alix, a protein that binds to LBPA-containing bilayers to stabilize LBPA levels in LEs. Based on our data, we propose that intra-endosomal trafficking mediated by LBPA significantly contributes to PS-ASO productive intracellular release.

MATERIALS AND METHODS

Antibodies, siRNAs, ASOs and quantitative real-time PCR (qRT-PCR) primer probe sets are described in Supplementary Data.

Cell culture, transfection, PS-ASO free uptake and activity assay

A431, HeLa, HepG2, MIA PaCa and Huh7 cells were grown according to the protocols provided by the American Type Culture Collection (ATCC, Manassas, VA, USA) (6). Cells were seeded at 70% confluency 1 day before transfection or drug treatment. siRNAs were transfected at 3 nM final concentration using RNAiMAX (Life Technologies, Carlsbad, CA, USA), according to the manufacturer's protocol. At 48 h after siRNA transfection, cells were re-seeded in either 96-well plates or collagen-coated dishes (MatTek, Ashland, MA, USA) at 50% confluency. Cells were incubated with PS-ASOs diluted to final concentration for 16 h, and then the PS-ASO activity assay or immunofluorescence analysis was performed.

RNA preparation and qRT-PCR

Total RNA was prepared using an RNeasy mini kit (Qiagen, Valencia, CA, USA) from cells grown in 96-well plates (around 10 000 cells per well). qRT-PCR using TaqMan primer probe sets were performed essentially as described previously (16). Briefly, ∼50 ng total RNA in 5 μl water was mixed with 0.3 μl primer probe sets containing forward and reverse primers (10 μM of each) and fluorescently labeled probe (3 μM), 0.3 μl RT enzyme mix (Qiagen), 4.4 μl RNase-free water, and 10 μl of 2× PCR reaction buffer in a 20 μl reaction. Reverse transcription was performed at 48°C for 10 min, 40 cycles of PCR were conducted at 94°C for 20 s and 60°C for 20 s using the StepOne Plus RT-PCR system (Applied Biosystems, Phoenix, AZ, USA). The mRNA levels were normalized to the amount of total RNA present in each reaction as determined for duplicate RNA samples by Ribogreen assay (Life Technologies).

Immunofluorescence staining

Cells were fixed with 4% paraformaldehyde for 30 min at room temperature and were permeabilized with 0.05% saponin (Sigma) in PBS for 5 min. Cells were treated with blocking buffer (1 mg/ml BSA in PBS) for 30 min and then incubated with primary antibodies (1:100–1:200 in blocking buffer) at room temperature for 2–4 h or at 4°C overnight. After three washes using 0.1% Triton in PBS, cells were incubated with fluorescently labeled secondary antibodies (1:200 in blocking buffer) at room temperature for 1–2 h. After washing, slides were mounted with Prolong Gold anti-fade reagent with DAPI (Life Technologies) and imaged using a confocal microscope (Olympus FV-1000). Co-localization between PS-ASOs and different organelles was analyzed using software of the FV10-ASW 3.0 viewer. Image intensities were also quantitated using the same software.

Protein isolation and western blotting

Cells were lysed, and samples were incubated at 4°C for 30 min in RIPA buffer (50 mM Tris–HCl, pH 7.4, 1% Triton X-100, 150 mM NaCl, 0.5% sodium deoxycholate and 0.5 mM EDTA). Proteins were separated by PAGE using 6% to 12% NuPAGE Bis-Tris gradient Gels (Life Technologies) and electroblotted onto PVDF membranes using the iBLOT transfer system (Life Technologies). The membranes were blocked with 5% non-fat dry milk in PBS at 4°C for 30 min. Membranes were then incubated with primary antibodies (Supplementary Data) at room temperature for 1 h. After three washes with PBS, the membranes were incubated with appropriate HRP-conjugated secondary antibodies (1:2000) at room temperature for 1 h to develop the image using ECL reagents (Abcam, Cambridge, MA, USA).

Flow cytometry

Indicated Cy3-labeled PS-ASO was added to A431 cell culture. After 3 h, cells were washed with PBS, trypsinized

and resuspended in PBS supplemented with 3% fetal bovine serum for analysis by flow cytometry using a BD Biosciences CellQuest Pro system (BD Biosciences, San Jose, CA, USA).

RESULTS

Kinetics of PS-ASOs uptake and activity

Given that PS-ASOs are internalized and transported along the endocytic pathways, PS-ASO activity could be determined either by levels of uptake or levels of intracellular release. To evaluate these two possibilities, we first performed kinetic studies on PS-ASO uptake and activity during a time course of 24 h in human epidermoid carcinoma A431 cells. The levels of uptake were determined by flow cytometry using different concentrations of Cy3-labeled PS-ASOs (IONIS ID 446654, see Supplementary Data for sequence and chemical modifications). Activity was determined by quantification of the RNAs, *Drosha* or *Malat1*, targeted by the two PS-ASOs (IONIS ID 395254 for *Malat1;* IONIS ID 25690 for *Drosha*), at different time points. Uptake of Cy3-labeled PS-ASO increased in a concentration-dependent manner as a function of time and was not saturated at the 24-h time point (Figure 1A and B). Activity was not detected for either *Drosha*- or *Malat1*-targeted PS-ASOs until 8 h after the PS-ASO treatment (Figure 1C and D). The uptake of PS-ASO increased ∼2 folds from 8 to 16 h post PS-ASO treatment, but the IC_{50} values dropped ∼10-fold during this time period (Figure 1E). These observations indicate that there is a significant delay from the time that PS-ASOs are internalized to the time that PS-ASOs reach their RNA targets.

To further understand the relationship between PS-ASO uptake and antisense activity, we analyzed uptake and activity in different human cell lines. Similar kinetics of PS-ASO uptake and activity were observed in another human cell line, MIA PaCa cells, upon free uptake (Supplementary Figure S1A). PS-ASOs are active in human A431 cells, less active in human HeLa and HEK cells and least active in human HepG2 and Huh7 cells; however, uptake levels of PS-ASOs were comparable in A431, HeLa and HepG2 cells (data not shown). Taken together, these observations indicate that the amount of PS-ASO internalized is not directly correlated with activities as measured by RNA target reduction and that the rate limiting step of PS-ASO to gain its activity is PS-ASO intracellular release, and not cellular uptake.

PS-ASO cargos bud as ILVs inside EEs and LEs in live cells

Previously, we reported that productive PS-ASO release mainly occurs after the PS-ASOs reach LEs/MVBs (8). To understand the mechanisms of productive PS-ASO release from LEs, we overexpressed a constitutively active form of Rab5, Rab5(Q79L), which impairs endosomal trafficking and induces the formation of enlarged endosomes that contain ILVs (17,18). If PS-ASOs are cargos that bud inward endosomes, they are expected to be inside enlarged endosomes with outer membranes labeled by RAB5(Q79L) (19). To test that possibility, HeLa cells overexpressing RAB5(Q79L)-GFP were treated with Cy3-labeled PS-ASO (IONIS ID 446654) for 4 h. PS-ASOs were indeed detected in dot-like structures inside the lumen of enlarged endosomes marked by RAB5(Q79L)-GFP (Figure 2A).

HeLa cells that overexpressed RAB7a-GFP were next incubated with Cy3-PS-ASO and then treated with the PIKfyve inhibitor YM201636 to enlarge LEs (20). Under these conditions, the fluorescently labeled PS-ASOs were also observed inside the lumen of enlarged LEs and concentrated in punctate structures with outer membranes marked by RAB7a-GFP (Figure 2B). Similar localization patterns were also observed in the enlarged EEs marked by Rab5 in Hela cells treated with YM201636 (Supplementary Figure S2). These observations confirm that PS-ASO cargos are able to bud as ILVs inside EEs and LEs in live cells.

ILVs can be labeled by a fluorescent lipid analog *N*-(lissamine rhodamine B sulfonyl)-phosphatidylethanolamine (N-Rh-PE) during membrane fusion events along the endocytic pathway (21). HeLa cells that overexpressed RAB5(Q79L)-GFP were co-treated with N-Rh-PE and Cy5-labeled PS-ASO (IONIS ID 851810) for 4 h. As expected, N-Rh-PE labeled ILVs inside enlarged LEs, and some co-localization with PS-ASO was observed in live cells (Figure 2C).

Internalized ligands tend to dissociate from receptors at either EEs or LEs due to the acidic environment of EEs and LEs (9). As PS-ASOs can be considered as ligands, it was surprising to find that PS-ASOs are mainly concentrated in ILVs. We then compared the localization pattern of PS-ASOs with other ligands such as LDL and transferrin in cells that overexpressed RAB5(Q79L)-GFP. LDL and transferrin accumulated in enlarged endosomes marked by RAB5(Q79L)-GFP. In contrast to PS-ASO, which is present in a punctate pattern, LDL or transferrin showed a diffuse pattern inside of LEs (Figure 2D). This difference in localization pattern suggests that LDL and transferrin are freed from receptors, whereas PS-ASOs are still tied up with either receptors or certain subcellular structures in LEs after internalization. There are at least two possible explanations for this. One is that PS-ASOs bind tightly to receptors or receptor-like proteins, and these complexes do not readily dissociate in EEs or LEs. The other is that PS-ASOs, either with or without binding proteins, may undergo changes in topology to translocate into the lumen of ILVs, which might result in PS-ASO release from ILV upon its fusion with the limiting membrane of the LEs (22).

PS-ASOs co-localize with LBPA-containing ILVs inside LEs

LBPA is abundant in the ILVs of LEs but not in EEs, reflecting active membrane deformation of LEs (23). To test whether PS-ASOs are present in LBPA-containing ILVs of LEs, we analyzed the cellular localization of Cy3-labeled PS-ASO (IONIS ID 446654) in HeLa cells stained for EEA1, a marker of EEs (24), and for LBPA over a time course from 0.5 to 8 h after PS-ASO addition to cells. Co-localization of PS-ASO with EEA1 peaked at 0.5 h. By 2 h, the majority of PS-ASO was co-localized with LBPA (Figure 3A). The quantitation of co-localization between PS-ASOs and LBPA indicates that more than 80% PS-ASOs were present in LBPA-positive organelles after cells were incubated with PS-ASOs for 2 h or longer (Supplementary

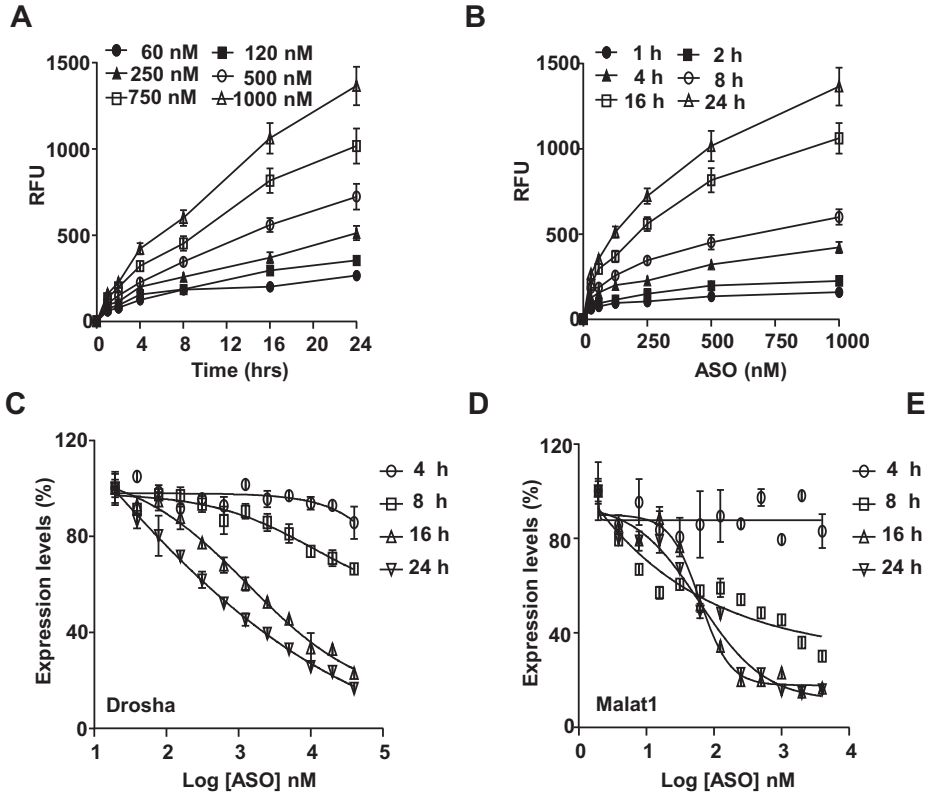

E

	IC50 (nM) (Drosha)	IC50 (nM) (Malat1)
4 h	N.A	N.A
8 h	11000±460	1200±98
16 h	1300±98	65±8
24 h	300±20	21±2

Figure 1. Activity of PS-ASOs through free uptake is mainly determined by intracellular release. (A and B) Intracellular fluorescence of Cy3-PS-ASO was quantified by flow cytometry to determine uptake (RFU) as a function of time at indicated given PS-ASO concentrations (**A**) and uptake (RFU) as a function of PS-ASO concentration at indicated time points (**B**). (C and D) Expression of *Drosha* (**C**) and *Malat1* (**D**) RNAs as a function of PS-ASO concentration at indicated time points quantified by qRT-PCR. Data are relative to no PS-ASO control. The error bars represent standard deviations from three independent experiments. (**E**) Values of IC_{50} were calculated from data plotted in panels based on a non-liner regression model.

Figure S3A). These results suggest that PS-ASOs can traffic to ILVs containing LBPA. The kinetics of PS-ASO localization to LBPA-containing ILVs also suggests a delay from the time that PS-ASOs are internalized to the time that PS-ASOs reach LEs to release.

To further confirm that PS-ASOs are co-localized with LBPA at ILVs inside LEs, we analyzed the cellular localization of LBPA and PS-ASO in cells overexpressing RAB5(Q79L). Cells were treated with Cy3-labeled PS-ASOs for 8 hours and then stained with LBPA antibody. PS-ASOs were observed in dot-like structures mainly present inside these enlarged endosomes as shown in Figure 2A and Figure 2C**.** LBPA was also detected in structures, likely ILVs, inside these enlarged endosomes (Figure 3B). Some PS-ASOs were clearly co-localized with structures stained by LBPA inside LEs. When the experiment was performed with Cy5-labeled PS-ASO, a similar co-localization of Cy5-PS-ASO and LBPA was also observed (data not shown); arguing that localization of the PS-ASO is not influenced by the fluorescent tag. The localization of proteins known to be present in ILVs, including mannose-6 phosphate receptor 1 and CD63 (25), was also examined in HeLa cells that overexpressed RAB5(Q79L)-GFP. Co-localization between PS-ASOs and these endocytic receptors was also observed (Figure 3C and Supplementary Figure S3B). Taken together, these observations suggest that some, if not all, PS-ASOs traffic to LBPA-containing ILVs inside LEs.

LBPA plays an indispensable role in regulating PS-ASO activity

The biogenesis of ILVs starts at EEs, which is mainly mediated by ESCRT protein complexes (25). To determine the role of ESCRT proteins in regulating PS-ASO activity, we reduced two major components in ESCRT, HRS (Hepatocyte Responsive Serum phosphoprotein) in ESCRT0 or TSG101 (Tumor Susceptibility Gene 101) in ESCRTI (25) using siRNAs targeting *HRS* or *TSG101*. The siRNAs decreased *HRS* or *TSG101* protein levels by >90% (Figure 4A and Figure 4B). Reduction of *HRS* or *TSG101* had no significant effect on PS-ASO activity, as demonstrated by qRT-PCR analyses for *Drosha* mRNA or *Malat1* RNA in control and *HRS* or *TSG101*-deficient cells incubated with the *Drosha*- or *Malat1*-specific PS-ASOs (Figure 4A and B). The experiments were repeated at least three times and similar resulted were observed. These results indicate that ESCRT proteins do not significantly contribute to productive release of PS-ASOs.

To examine the role of LBPA in PS-ASO activity, we used the monoclonal antibody (mAb, 6C4) to block the functionality of LBPA (13). LBPA-containing ILVs have been proposed to mediate substance release from ILVs through back fusion between limiting membranes and ILVs. LBPA antibody (mAb, 6C4) has been shown to deactivate this process (13). Pre-treatment with anti-LPBA antibody re-

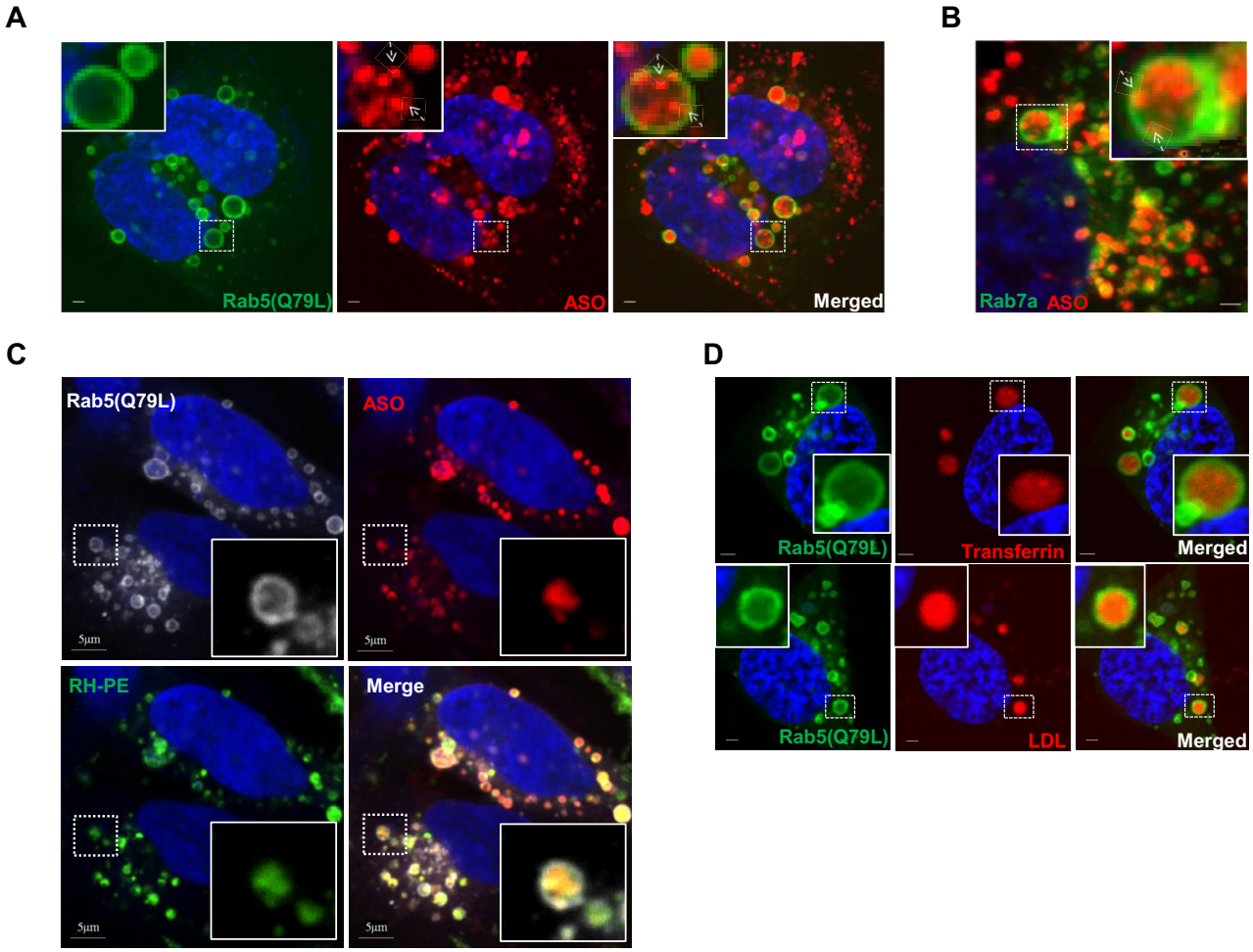

Figure 2. PS-ASO cargos bud as ILVs inside LEs in live cells. (**A**) Representative images of cells overexpressing RAB5(Q79L)-GFP (green) treated with 2 μM Cy3-labeled PS-ASO (red) for 4 h. The nuclei were stained with Hoechst 33342 (blue). Scale bar, 5 μm. (**B**) Representative merged images of cells overexpressing RAB7a-GFP (green) incubated with 2 μM Cy3-labeled PS-ASO (red) for 4 h followed by treatment with YM201636 for an additional 8 h. The nuclei were stained with Hoechst 33342 (blue). Scale bar, 5 μm. (**C**) Representative images of cells overexpressing RAB5(Q79L)-GFP (gray) and treated with Cy5-labeled PS-ASO (red) and N-Rh-PE (green) for 4 h. The nuclei were stained with Hoechst 33342 (blue). Scale bar, 5 μm. (**D**) Representative images of cells overexpressing RAB5(Q79L)-GFP (green) treated with Cy5-labeled-transferrin (red) or Alexa Fluor® 594-LDL (red) for 4 h. The nuclei were stained with Hoechst 33342 (blue). Scale bar, 5 μm.

sults in accumulation and inactivation of LBPA in LEs (26). A431 cells were pre-treated with anti-LBPA antibody or an IgG control and subsequently treated with either *Drosha*- or *Malat1*-specific PS-ASOs. As show in Figure 5A, anti-LBPA antibody reduced activities of both PS-ASOs. Since PS-ASOs are localized in LBPA-containing ILVs (Figure 3) and treatment of LBPA antibody decreases PS-ASO activities in cells, it is likely that PS-ASOs are productively released through the process of back fusion.

The small molecule U18666A treatment causes acute accumulation of cholesterol in LEs, which inhibits the activity of LBPA in membrane deformation (27). U18666A-treated cells have enlarged LEs and defects in intra-endosomal trafficking such as back fusion processes (28). We pre-treated A431 cells with U18666A for 6 h and then added *Drosha*- or *Malat1*-specific PS-ASOs. As shown in Figure 5B, U18666A significantly reduced activities of both PS-ASOs. This result suggests that LBPA-mediated intra-endosomal trafficking is important for the release of PS-ASOs from LEs.

LBPA does not influence uptake or endocytic trafficking of PS-ASOs to LEs

To evaluate the possibility that LBPA directly contributes to PS-ASO internalization, we analyzed the effect of LBPA inactivation on levels of PS-ASO cellular uptake. A431 cells treated with anti-LBPA antibody (50 μg/ml) or an IgG control were incubated with 1 μM Cy3-labeled PS-ASO for 3 h, and then samples were analyzed by FACS. The levels of internalized PS-ASOs were increased ∼20% in cells treated with anti-LBPA antibody compared with cells treated with an IgG control (Figure 5C). Similarly, treatment of cells with U18666A (2.5 μM) did not decrease internalization of Cy3-PS-ASOs (Figure 5D). These results indicate that decreased PS-ASO activities in cells treated with anti-LBPA

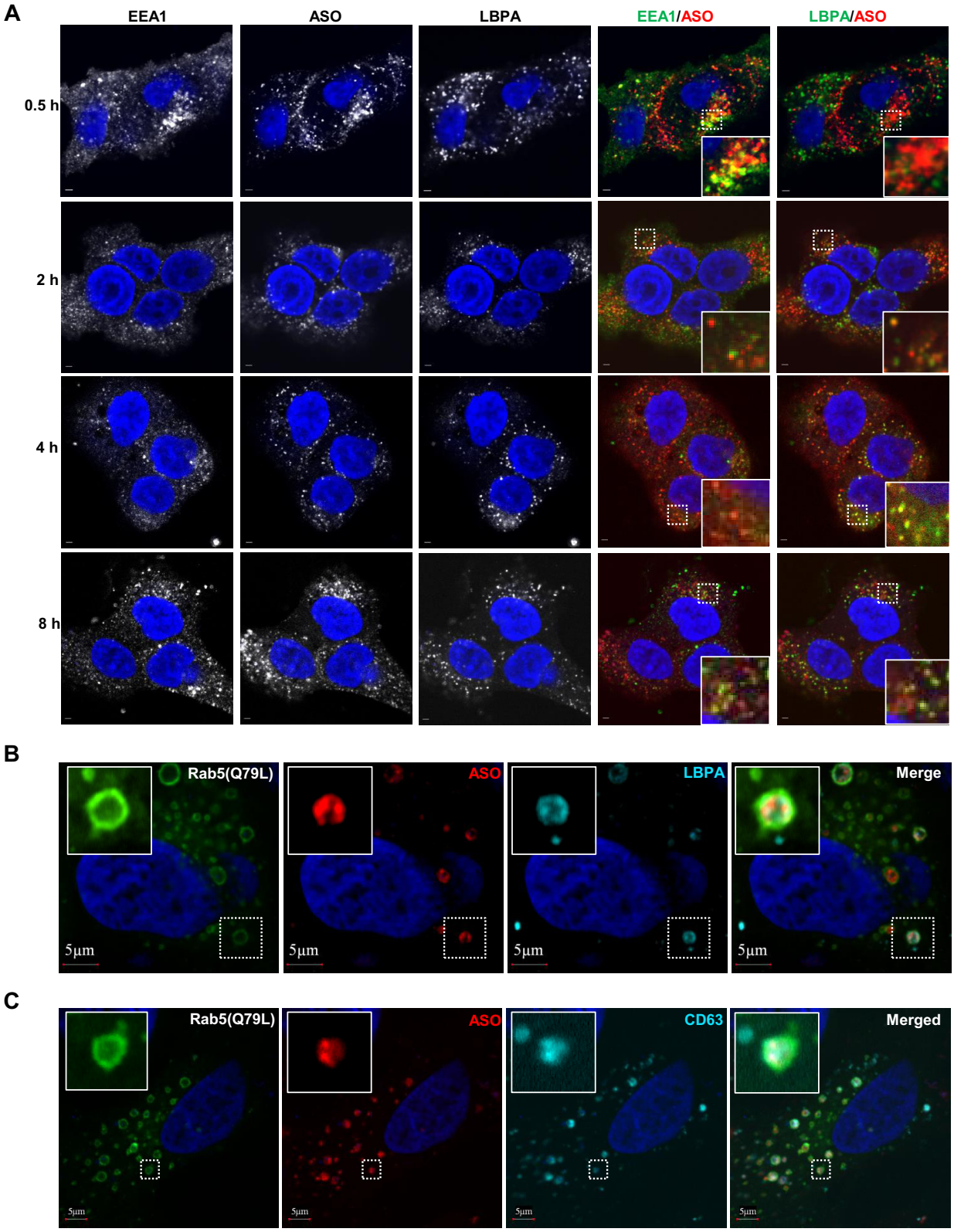

Figure 3. PS-ASOs are predominantly co-localized with LBPA-containing ILVs inside LEs. (**A**) Representative images of immunofluorescent staining for EEA1 (green) and LBPA (green) in HeLa cells incubated with Cy3-labeled PS-ASO (red) for the indicated times. The nuclei were stained with DAPI (blue). Enlarged images showed co-localization between PS-ASOs and EEA1 or LBPA in yellow, Scale bar, 5 μm. (**B**) Representative images of immunofluorescent staining for LBPA (cyan) in cells overexpressing RAB5(Q79L)-GFP (green) and treated with Cy3-PS-ASO (red). The nuclei were stained with DAPI (blue). Scale bar, 5 μm. (**C**) Representative images of immunofluorescent staining for CD63 (cyan) in cells overexpressing RAB5(Q79L)-GFP (green) and treated with Cy3-PS-ASO (red). The nuclei were stained with DAPI (blue). Scale bar, 5 μm.

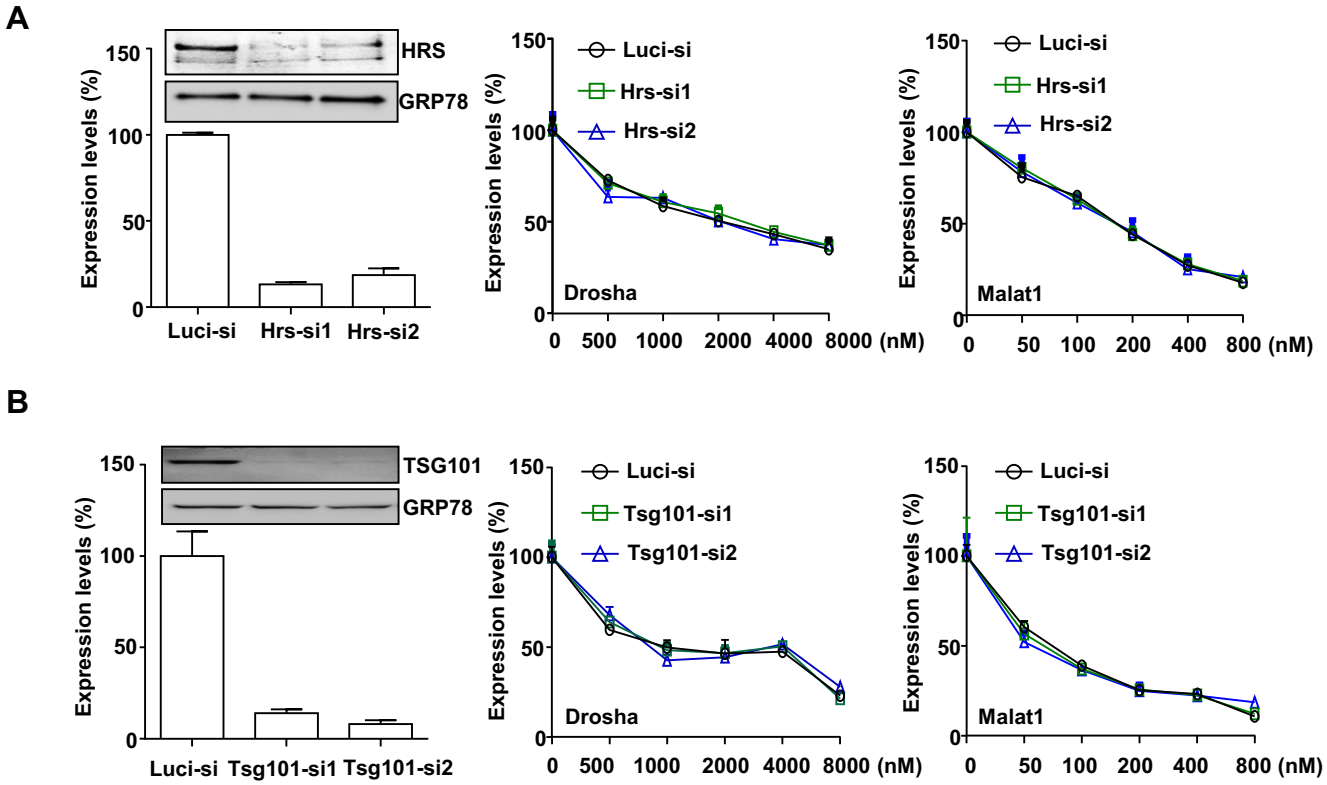

Figure 4. ESCRT proteins do not regulate PS-ASO activity. (**A**) A431 cells were treated with control siRNA targeting luciferase (Luc-si) or siRNAs targeting HRS as indicated. Left panel shows RNA and protein levels of HRS determined by qRT-PCR and Western analyses, respectively. RNA levels are relative to Luc-siRNA treated samples. GRP78 served as a Western loading control. Middle and right panels show data from cells treated with indicated siRNAs for 48 h and then incubated with PS-ASOs targeting either *Drosha* or *Malat1* for 16 h. *Drosha* and *Malat1* RNA levels were quantified using qRT-PCR. The error bars represent standard deviations from three independent experiments. (**B**) A431 cells were treated with control siRNA targeting luciferase (Luc-si) or siRNAs targeting TSG101 as indicated. Left panel shows RNA and protein levels of TSG101 determined by qRT-PCR and western analyses. RNA levels are relative to control siRNA treated samples. GRP78 served as a western loading control. Middle and right panels show data from cells treated with indicated siRNAs for 48 h and then incubated with PS-ASOs targeting either *Drosha* or *Malat1* for 16 h. RNA levels were quantified using qRT-PCR. The error bars represent standard deviations from three independent experiments.

antibody or U18666A are not attributable to decreased intracellular uptake of PS-ASOs.

Since PS-ASO release mainly occurs from LEs, delayed traffic of PS-ASOs to LEs could contribute to decreased PS-ASO release (8). Previously, we found that reduction of Annexin A2 delayed ASO trafficking from EEs to LEs as examined by PS-ASO co-localization in EEs or LEs/lysosomes 2 h after incubation (8). To test whether inactivation of LBPA affects endocytic trafficking of PS-ASOs to LEs, we analyzed the transport of PS-ASOs in cells pre-treated with anti-LBPA antibody. HeLa cells were treated with anti-LBPA antibody or an IgG control for 6 h. Cells were then incubated with 2 μM Cy3-labeled PS-ASOs for another 2 h and stained with EEA1, an EE marker, and LAMP1, a marker of late endosomes or lysosomes (31). The anti-LBPA antibody treatment increased the sizes of LEs/lysosomes with limiting membranes marked by LAMP1, as published before (Supplementary Figure S3) (29). However, quantification of PS-ASO-positive EEs (PS-ASOs and EEA1 co-staining) and PS-ASO-positive LEs or lysosomes (PS-ASO and LAMP1 co-staining) showed that the anti-LBPA antibody treatment did not alter the portions of EEs and LEs that contained PS-ASOs (Supplementary Figure S3). This result indicates that LBPA inactivation does not delay endocytic trafficking of PS-ASOs to LEs. Similar experiments conducted with cells pre-treated with 2.5 μM U18666A for 6 h followed by incubation with 2 μM Cy3-labeled PS-ASOs for 2 h showed that trafficking of PS-ASOs from EEs to LEs was not disrupted by U18666A treatment (data not shown). These data indicate that trafficking of PS-ASOs from EEs to LEs is not impaired in cells with LBPA inactivation.

Alix and NPC1 are important for PS-ASO activity

The protein Alix controls LBPA functions by binding to LBPA-containing bilayers to stabilize LBPA levels in LEs (15). To determine whether the function of LBPA in regulation of PS-ASO activity is also Alix dependent, we reduced the levels of Alix using siRNA and then evaluated PS-ASO activity. A431 cells were treated with two different siRNAs targeting Alix and both decreased Alix protein levels by >90% (Figure 6A). Similar to LBPA inactivation, reduction of Alix significantly decreased PS-ASO activities (Figure 6A). This result was independently confirmed in MHT cells (internal communication with Dr. Eric Koller). This observation further supports our hypothesis that LBPA plays a positive regulatory role in PS-ASO re-

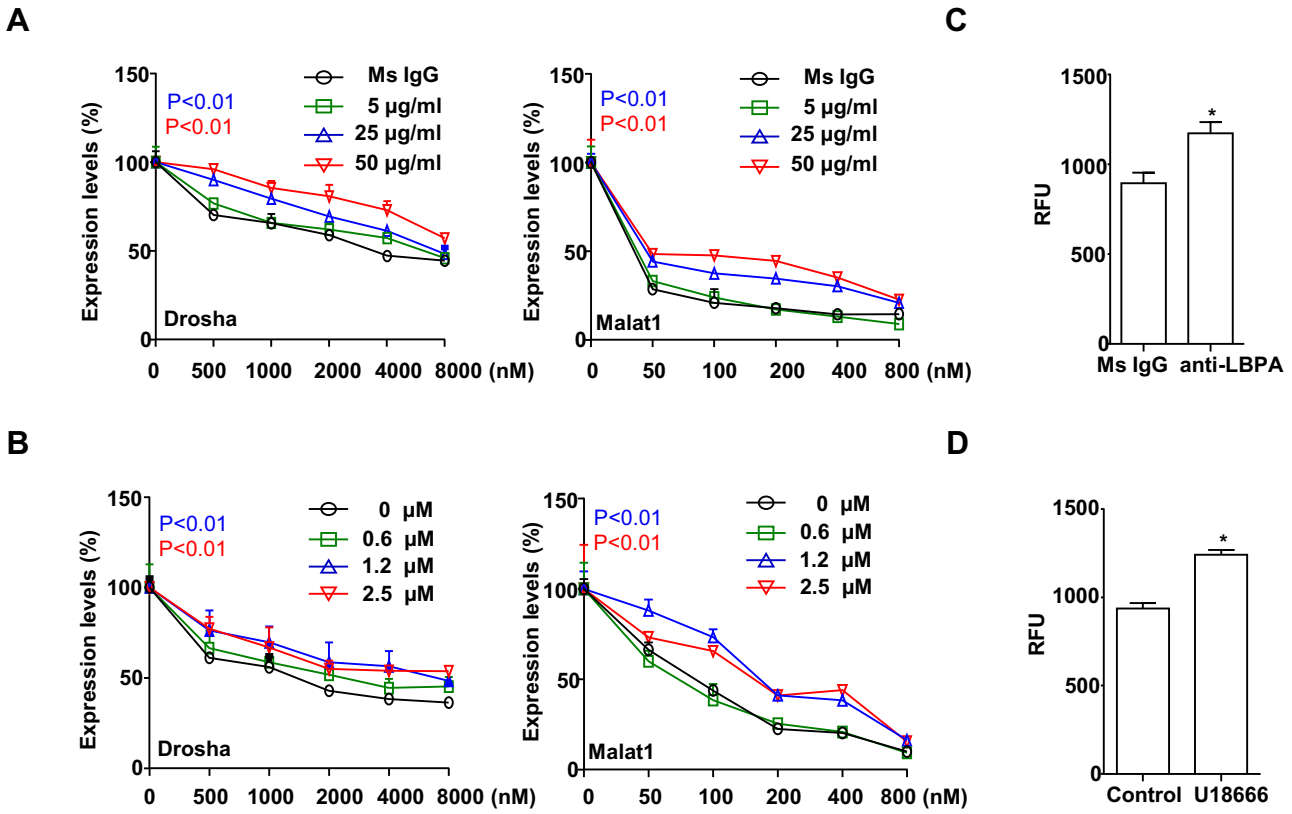

Figure 5. LBPA plays an indispensable role in regulating PS-ASO activity. (**A**) A431 cells were pre-treated with different concentrations of anti-LBPA antibody or an mouse IgG (Ms IgG) as control for 6 h, followed by incubation with PS-ASOs targeting *Drosha* or *Malat1* RNA for 16 h. The levels of *Drosha* and *Malat1* RNAs were determined by qRT-PCR. The error bars represent standard deviations from three independent experiments. *P* (in blue, 25 μg/ml) <0.01 versus Ms IgG; *P* (in red, 50 μg/ml) <0.01 versus Ms IgG. (**B**) A431 cells were pre-treated with different concentrations of U18666A or control for 6 h, followed by incubation with PS-ASOs targeting *Drosha* or *Malat1* RNA for 16 h. The levels of *Drosha* and *Malat1* RNAs were determined by qRT-PCR. The error bars represent standard errors from three independent experiments. *P* (in blue, 1.2 μM) <0.01 versus Ms IgG; *P* (in red, 2.5 μM) <0.01 versus 0 μM. (**C**) A431 cells were pre-treated with 50 μg/ml anti-LBPA antibody or an IgG control for 6 h, followed by incubation with 1 μM Cy3-labeled PS-ASO for 3 h. PS-ASO uptake was analyzed by flow cytometry. The error bars represent standard errors from three independent experiments. *$P < 0.01$ versus Ms IgG. (**D**) A431 cells were pre-treated with 2.5 μM U18666A or ethanol as control for 6 h, followed by incubation with 1 μM Cy3-labeled PS-ASO for 3 h. PS-ASO uptake was analyzed by flow cytometry. The error bars represent standard deviations from 3 independent experiments. *$P < 0.01$ versus control.

lease from LEs to the cytoplasm or nucleus and shows that the release also requires Alix.

The protein NPC1 controls intracellular cholesterol mobilization and deletion of NPC1 phenocopies the treatment of U18666A and causes cholesterol accumulation in LEs (29). Reduction of NPC1 inhibits the activity of LBPA in membrane deformation (28). A431 cells were treated with two different siRNAs targeting NPC1. Reduction of NPC1 also decreased PS-ASO activities significantly, as measured by less reduction of RNAs targeted by the *Drosha*- or *Malat1*-specific ASOs (Supplementary Figure S4). This result confirms the importance of LBPA and its function in membrane deformation in PS-ASO release from LEs.

To rule out the possibility that Alix influences PS-ASO internalization, we also measured cellular uptake of Cy3-PS-ASOs in cells treated with siRNAs targeting Alix. FACS analyses indicated that reduction of Alix did not substantially change cellular uptake of PS-ASOs (Figure 6B), suggesting that Alix influences PS-ASO release from the endocytic pathway.

We previously showed that RNase H1 (30), P54nrb (31), HSP90 (32) and Annexin A2 (8) affect PS-ASO activities through different mechanisms. To dissect the function of Alix, we measured levels of these proteins by western blotting in cells treated with siRNA targeting Alix. Levels of these proteins were not changed in cells depleted of Alix (Figure 6C). These results indicate that the role of Alix in PS-ASO activity is independent of proteins previously shown to influence PS-ASO activity.

Alix reduction does not delay endocytic trafficking of PS-ASOs to LEs

In addition to controlling LBPA activity, Alix also regulates endocytic trafficking to LEs and exosome biogenesis (19). We therefore examined whether Alix functions in endocytic trafficking of PS-ASOs to LEs. A431 cells were treated with Alix siRNA for 48 h and were then incubated with 2 μM Cy3-labeled PS-ASOs (IONIS ID 446654) for another 2 h. Cells were stained with EEA1 and LAMP1 to monitor the kinetics of PS-ASO trafficking to LEs. Unlike the anti-LBPA antibody treatment, Alix reduction did not

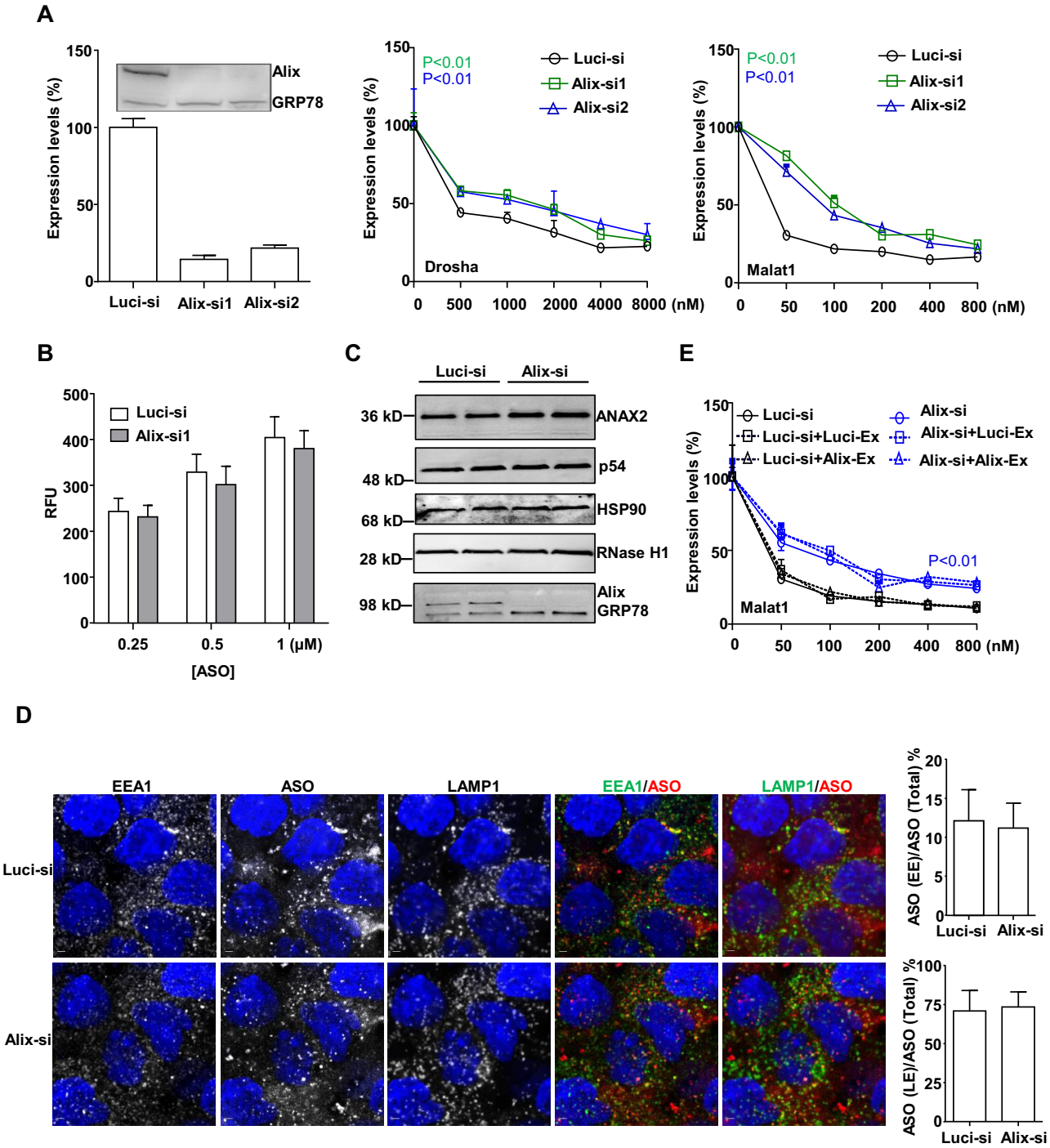

Figure 6. Alix is important for PS-ASO activity. (**A**) A431 cells were treated with control (Luc-si) or siRNAs targeting Alix as indicated. Left panel shows RNA and protein levels of Alix determined by qRT-PCR and western analyses. RNA levels are relative to Luc-siRNA treated samples. GRP78 served as a loading control. Middle and right panels show data from cells treated with siRNAs targeted Alix for 48 h and then incubated with PS-ASOs targeting either *Drosha* or *Malat1* for 16 h. RNA levels were quantified using qRT-PCR. The error bars represent standard deviations from three independent experiments. $P < 0.01$ (in green, Alix-si1) versus Luci-si; $P < 0.01$ (in blue, Alix-si2) versus Luci-si; (**B**) A431 cells treated with control siRNA or siRNA targeting Alix (Alix-si1) were incubated with Cy3-PS-ASOs for 3 h. PS-ASO uptake was analyzed by flow cytometry. The error bars represent standard deviations from three independent experiments. (**C**) Western analyses for ANXA2, P54nrb, HSP90, RNase H1 and Alix proteins in cells treated with control or Alix siRNAs for 48 h. GRP78 served as a loading control. (**D**) Representative images of immunofluorescent staining for EEA1 (green), and LAMP1 (green) in A431 cells incubated with Cy3-labeled PS-ASOs (red) for 2 h. Scale bar, 5 μm. The PS-ASO-positive EEs or LEs were counted in 20 cells, and the percentage of the PS-ASO-positive EEs or LEs was calculated relative to the total numbers of the PS-ASO-positive organelles. (**E**) A431 cells treated with control (Luc-si) or siRNA targeting Alix (Alix-si1) were incubated with PS-ASOs targeting *Malat1* for 12 h, followed by the replacement of fresh media without PS-ASOs for another 12 h to allow exosome secretion. Exosomes from either control or Alix-si1-treated cells were added to cells, which were co-treated with *Malat1*-specific PS-ASOs at different doses. The RNA levels were quantified using qRT-PCR. The error bars represent standard deviations from three independent experiments. $P < 0.01$ (in blue, either of Alix-si curves) versus either of Luci-si curves.

increase the sizes of LEs (Figure 6D). Quantification of the co-localization between EEs and PS-ASOs or LEs and PS-ASOs showed that reduction of Alix did not reduce the percentage of PS-ASO-containing LEs (Figure 6D). This result indicates that Alix is not essential for endocytic trafficking of PS-ASOs to LEs.

Exosome is known to transfer productive siRNAs between cells (33). It is possible that PS-ASOs can be trafficked through exosomes across cells, which, in turn, contributes to the productive release of PS-ASOs. We then examined the function of Alix in the biogenesis of PS-ASO-containing exosomes (19). A431 cells were first treated with control or Alix-targeted siRNA for 36 h to efficiently reduce Alix levels. Cells were then incubated with media containing *Malat1*-specific PS-ASOs for another 12 h, followed by the replacement of fresh media without PS-ASOs. Cells were further incubated with the fresh media for another 12 h to allowed sufficient secretion of PS-ASO-containing exosomes into the media. Thereafter, the media containing PS-ASO exosomes from either control cells or Alix-reduced cells were collected, and added to cells that were co-treated with *Malat1*-specific PS-ASOs at different doses for 16 h. If PS-ASO activity is, at least in part, attributable to PS-ASO containing exosomes, PS-ASO activity should be elevated in cells with co-treatment of PS-exosome containing media. Interestingly, addition of the media containing exosomes, from either control or Alix-reduced cells, did not increase PS-ASO activity, suggesting that the exosomes do not contain sufficient productive PS-ASOs to increase activity (Figure 6E). These observations argue against the possibility that Alix contributes to PS-ASO activity by affecting PS-ASO exosome secretion. Therefore, it is most likely that Alix positively regulates PS-ASO activities by controlling the levels or stability of LBPA in LEs.

Alix reduction decreases LBPA levels and diminishes co-localization of LBPA with PS-ASOs

To determine if reduction of Alix decreases PS-ASO activities via destabilization of LBPA, we examined levels of LBPA and the incidence of co-localization between LBPA and PS-ASOs (28). We monitored LBPA staining pattern and quantified LBPA staining intensity in control cells and cells deficient in Alix. A431 cells were treated with control or Alix-targeted siRNA for 48 h and then incubated with 2 μM Cy3-labeled PS-ASOs for 4 h. The fluorescent intensity of LBPA staining was quantified and normalized to the intensity of LAMP1. Compared to control cells, cells depleted of Alix had a ∼40% decrease in LBPA signal, indicating that Alix reduction indeed decreases LBPA levels in LEs (Figure 7A and B). This result is consistent with previous studies showing that Alix is important for maintaining LBPA levels in LEs (15,28). Although LBPA staining is weak, after signal being intensified, the incidence of co-localization between LBPA and PS-ASOs did not significantly decrease in Alix-deficient cells compared to control cells (Figure 7C). This observation is consistent with the fact that reduction of Alix did not affect PS-ASO trafficking from EEs to LEs as LBPA is also a marker of LEs (Figure 6D).

To further examine how Alix reduction influences PS-ASO activity through LBPA, we compared localization pattern of LBPA in control cells and Alix-deficient cells after the treatment of PIKfyve inhibitor YM201636. Cells were incubated with 2 μM Cy3-labeled PS-ASOs for 4 h, which allowed PS-ASOs to traffic to ILVs before the treatment of YM201636 for 8 h to enlarge the sizes of LEs. Cells were further stained with LBPA and LAMP1. YM201636 treatment increased the sizes of LEs, resulting in a distinguishable inner space surrounded by LAMP1-stained limiting membranes (Figure 7D). In control cells, LBPA was mainly co-localized with PS-ASOs inside these enlarged endosomes, likely ILVs. In cells, deficient in Alix, LBPA staining signal was weak (Figure 7A) but after being intensified, it was mainly detected in the limiting membranes with comprised co-localization with PS-ASOs inside the enlarged endosomes (Figure 7D). Interestingly, in Alix-reduced cells, PS-ASOs were still predominantly observed inside enlarged LEs (Figure 7D), suggesting that inward budding of PS-ASOs is not solely dependent on either Alix or LBPA in LEs. However, loss of Alix appears to decrease LBPA levels at PS-ASO containing ILVs inside LEs. These LBPA-deficient ILVs may be unable to fuse with limiting membranes, preventing PS-ASO release from LEs.

DISCUSSION

Previously we showed that productive PS-ASO release mainly occurs from LEs (8). In the present study, we demonstrated a requirement of LBPA for PS-ASO release from LEs. PS-ASOs exit EEs rapidly after internalization and are further sorted to LBPA-containing ILVs in LEs. LBPA is important for PS-ASO release from LEs into the cytoplasm or nucleus where the PS-ASOs access RNA targets (Figure 8).

Our kinetic studies indicate that there is a significant delay from the time that PS-ASOs are internalized to the time that PS-ASOs reach their RNA targets. This time lapse allows sufficient PS-ASOs to traffic into and release from LEs, which is reflected as co-localization between LBPA and PS-ASOs. In addition, the effects of PS-ASOs gradually increase over time, suggesting a continuous release of PS-ASOs at low levels from LBPA-containing LEs. Interestingly, the pharmacological effects of PS-ASOs are highly varied among different cell types. Even when uptake levels of PS-ASOs are comparable, activities of PS-ASOs can be rather different between cell types. These cells, presumably, all contain LBPA in their LEs, suggesting that there are different limiting factors that contribute to PS-ASO activity due to LBPA-containing LEs and that other pathways may also contribute to PS-ASO activity.

Internalized ligands such as LDL and transferrin tend to dissociate from receptors and are present in diffuse states inside LEs. PS-ASOs, however, were detected as punctate structures co-localized with ILVs inside LEs. This observation suggests that lease some PS-ASOs are still associated with receptors and sorted to ILVs inside LEs after internalization. It is well known that PS-ASO uptake can occur through receptor-mediated endocytosis at low concentrations (<1 μM) (2). Receptors such as integrins (e.g. Mac-1/CD18) (34), G-protein-coupled receptor (35), and scavenger receptors (Stabilin1 and 2) (36) have been implicated in PS-ASO uptake. The route of internalization through dif-

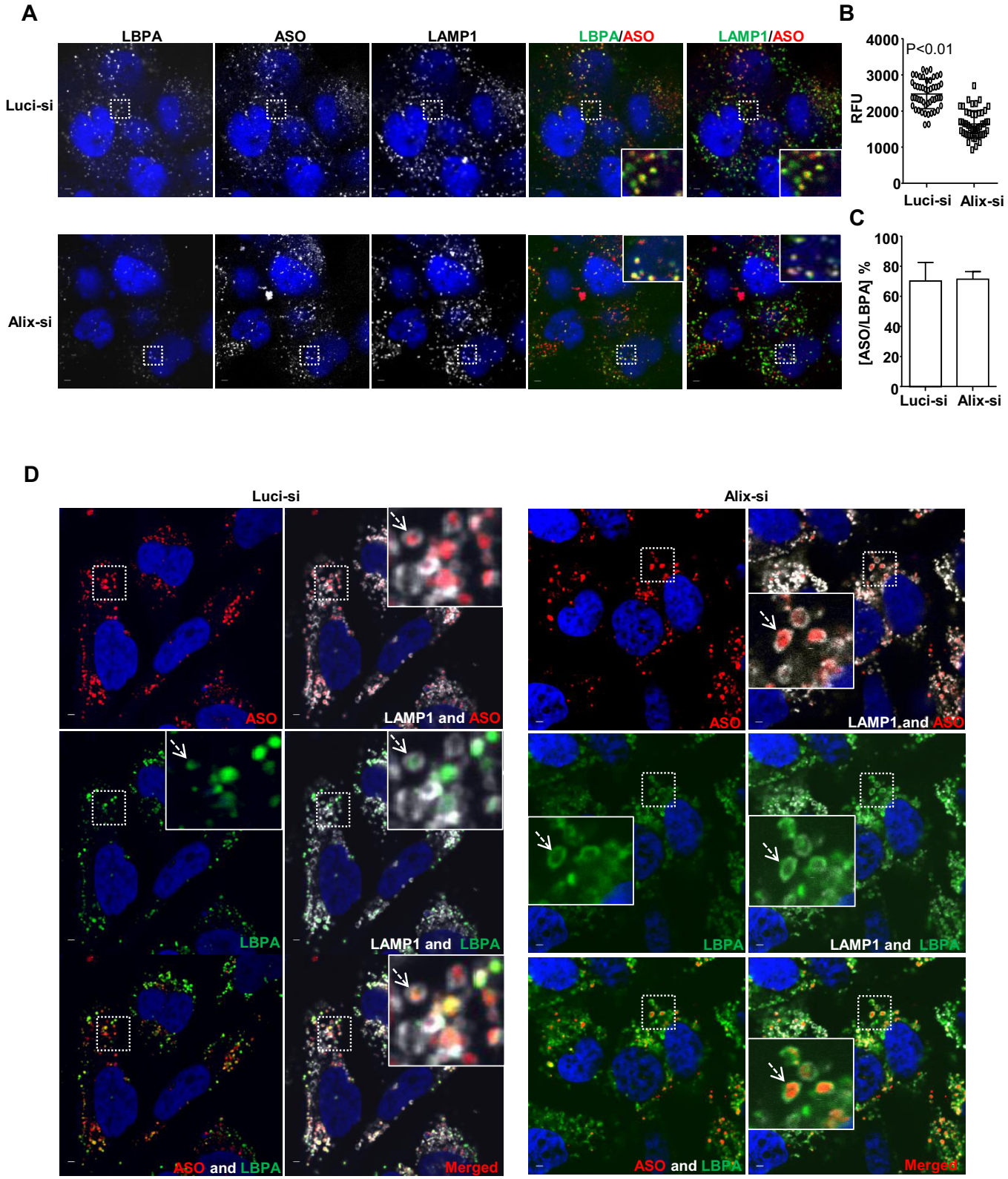

Figure 7. Alix reduction decreases LBPA levels and diminishes co-localization of LBPA with PS-ASOs at ILVs. (**A**) Representative images of immunofluorescent staining for LBPA (green) and LAMP1 (green) in control- or Alix-siRNA treated A431 cells, which were further incubated with Cy3-labeled PS-ASOs (red) for 2 h. The nuclei were stained with DAPI (blue). Scale bar, 5 μm. (**B**) Intensities of LBPA in 20 LEs from each of 15 cells were quantified and normalized to intensities of LAMP1 using FV10-ASW 3.0 viewer. $P < 0.01$, Alix-si versus Luci-si. (**C**)The PS-ASO-positive organelles co-stained with LBPA were also counted in 20 Luci- or Alix-siRNA treated A431 cells. The percentage of the organelles positive for both PS-ASOs and LBPA was calculated relative to the total numbers of the PS-ASO-positive organelles. (**D**) Representative images of immunofluorescent staining for LBPA (green) and LAMP1 (gray) in Luci- or Alix-siRNA treated HeLa cells, which were further treated with YM201636 after the incubation with Cy3-labeled PS-ASOs (red) for 4 h. The nuclei were stained with DAPI (blue). Scale bar, 5 μm.

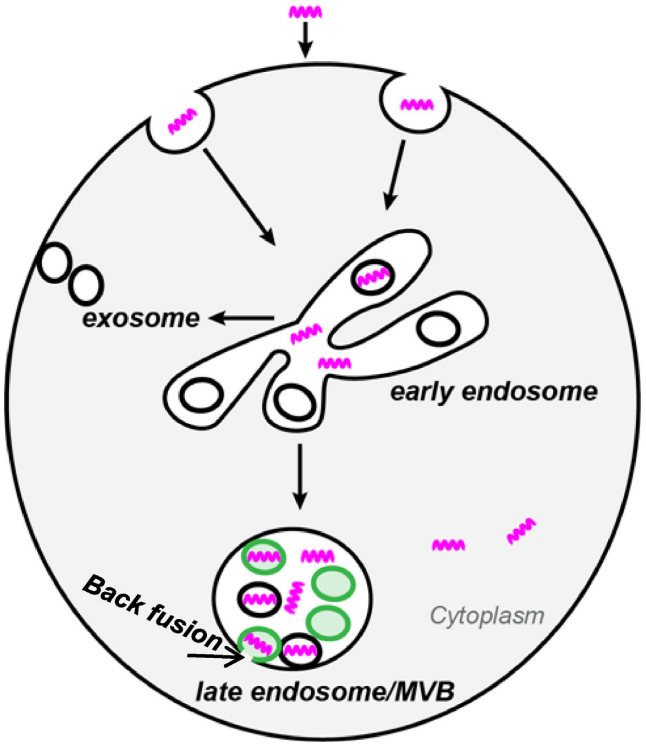

Figure 8. Proposed model of LBPA-mediated PS-ASO trafficking and release. PS-ASOs (purple twists) traffic along endocytic pathways from EEs to LEs. In EEs, PS-ASOs begin to be sorted into ILVs. In LEs, PS-ASOs are further sorted into ILVs containing LBPA (green). The deformation potential of LBPA drives the fusion between ILVs and limiting membranes to promote the productive PS-ASO release from LEs into the cytoplasm.

ferent surface proteins appears to affect the pharmacological activity of PS-ASO (37). Uptake of PS-ASOs preferentially by some pathways tends to increase PS-ASO activities (37), suggesting that these surface proteins can facilitate PS-ASO release from LEs more efficiently than others. It is possible that these proteins can promote sorting of PS-ASOs to ILVs, which, in turn, leads to the release of PS-ASOs through back fusion mechanism.

There are two major mechanisms that are involved in ILV formation. One is mediated by the ESCRT protein machinery and the other by LBPA (9). These two mechanisms can independently control ILV formation depending on substances to be sorted (38). ESCRT proteins do not appear to play important roles in productive release of PS-ASOs because inhibition of HRS or TSG101 expression did not alter PS-ASO activities. ILVs are observed in cells even lacking all components in the ESCRT protein machinery (25,39). It appears that sorting PS-ASO cargos to ILVs was not solely dependent on LBPA because in Alix reduced cells, PS-ASOs were also observed inside LEs, likely ILVs. Therefore, the mechanism that mediates PS-ASO sorting into ILVs needs further investigation.

LBPA is uniquely present at both ILV membranes and limiting membranes of LEs (23). LBPA is important for membrane deformation and fusion (25) and is critical in the back fusion that results in viral particle release from LEs to cytoplasm (26). We have shown that PS-ASOs were sorted to LBPA-containing-ILVs in LEs and that deactivation or destabilization of LBPA reduced PS-ASO activity. It is not known whether LBPA at ILV membranes or at limiting membranes or both contributes to productive PS-ASO release from LEs. Nonetheless, in Alix reduced cells, LBPA was mainly localized in limiting membranes while PS-ASO activity was reduced. It appears that LBPA at ILV membranes plays a major role in late endosomal release of PS-ASOs.

Back fusion is a well-known mechanism by which LBPA mediates substance release from LEs (15). Since deactivation of LBPA reduces PS-ASO activities, we speculate that back fusion results in productive PS-ASO release from LEs (Figure 8). Back fusion is the fusion between limiting membranes and enclosed ILVs (14). Upon back fusion, the cargo in the lumen of the ILV can be released into the cytoplasm (26). PS-ASOs were detected as punctate structures co-localized with ILVs rather than diffusely inside LEs, raising the possibility that through an unknown mechanism, PS-ASOs are able to enter the lumen of ILVs. If the sorting of PS-ASOs to ILVs is only mediated by interactions with PS-ASO binding receptor(s), retention of PS-ASOs at the outer membranes of ILVs through association with extracellular domains of receptor(s) may take place. Given the high propensity of PS-ASOs to bind to proteins, other proteins than receptor(s) could be involved in translocating PS-ASOs into the lumen of ILVs (37). Nonetheless, this mysterious process is the critical event that mediates topology changes of PS-ASOs into the lumen of ILVs for release through back fusion. Further study is necessary to elucidate the mechanistic details in the process.

Different models have been proposed to explain PS-ASO escape from LEs (22). One model is that protein binding to certain lipid domains could create temporary curvature of membranes with increased permeability, which leads to PS-ASO release (5,40,41). Our previous study identified ANXA2 as such a protein that may facilitate PS-ASO release from LEs (8). Another model is that membrane fission or fusion during the intracellular trafficking process could lead to the formation of non-bilayer lipid domains with increased membrane permeability, which would allow PS-ASO release (5,14,42). Our present study emphasized the importance of a membrane fusion event, back fusion from ILVs to LEs, in the release of PS-ASOs. Thus, it appears that membrane fission or fusion process plays an important role in PS-ASO release from LEs. Nevertheless, our data do not exclude the possibility that other pathways contribute to PS-ASO activity.

Some small molecules, such as Ritro-1 (43), UNC7938, UNC7832 and UNC7854 (44) can dramatically enhance PS-ASO activity via novel mechanisms involving release from LEs or redistribution to their action sites. Although those molecules do not affect sub-cellular organization and intracellular trafficking in general, they are relatively low potency, low stability and poor water solubility to use as drugs. Therefore, small molecules need further development if they are to be used to enhance PS-ASO actions through highly selective modulation of intracellular processing (44). On the other hand, based on our studies, it is conceivable that the pharmacological effect of PS-ASOs can be further improved by engineering chemical modifications that affect binding to key proteins involved in PS-ASO trafficking (37).

Back fusion could be one of the mechanisms that mediate productive PS-ASO release from LEs. Further understanding of the release pathways will guide development of strategies to improve the pharmacological effects of PS-ASO-based drugs (7).

SUPPLEMENTARY DATA

Supplementary Data are available at NAR Online.

ACKNOWLEDGEMENTS

We thank Dr. C. Frank Bennett and Dr. Wen Shen for stimulating discussions. We thank Dr Eric Koller for his supporting results. We thank Tracy Reigle for the graphic preparation.

FUNDING

Internal funding from Ionis Pharmaceuticals. Funding for open access charge: Ionis Pharmaceuticals.
Conflict of interest statement. None declared.

REFERENCES

1. Bennett,C.F. and Swayze,E.E. RNA targeting therapeutics: molecular mechanisms of antisense oligonucleotides as a therapeutic platform. *Annu. Rev. Pharmacol. Toxicol.*, **50**, 259–293.
2. Beltinger,C., Saragovi,H.U., Smith,R.M., LeSauteur,L., Shah,N., DeDionisio,L., Christensen,L., Raible,A., Jarett,L. and Gewirtz,A.M. (1995) Binding, uptake, and intracellular trafficking of phosphorothioate-modified oligodeoxynucleotides. *J. Clin. Invest.*, **95**, 1814–1823.
3. Crooke,S.T. (2004) Progress in antisense technology. *Annu. Rev. Med.*, **55**, 61–95.
4. Juliano,R.L. and Carver,K. (2015) Cellular uptake and intracellular trafficking of oligonucleotides. *Adv. Drug Deliv. Rev.*, **87**, 35–45.
5. Juliano,R.L., Ming,X. and Nakagawa,O. (2012) Cellular uptake and intracellular trafficking of antisense and siRNA oligonucleotides. *Bioconjug. Chem.*, **23**, 147–157.
6. Koller,E., Vincent,T.M., Chappell,A., De,S., Manoharan,M. and Bennett,C.F. (2011) Mechanisms of single-stranded phosphorothioate modified antisense oligonucleotide accumulation in hepatocytes. *Nucleic Acids Res.*, **39**, 4795–4807.
7. Juliano,R.L., Ming,X., Carver,K. and Laing,B. (2014) Cellular uptake and intracellular trafficking of oligonucleotides: implications for oligonucleotide pharmacology. *Nucleic Acid Therap.*, **24**, 101–113.
8. Wang,S., Sun,H., Tanowitz,M., Liang,X.H. and Crooke,S.T. (2016) Annexin A2 facilitates endocytic trafficking of antisense oligonucleotides. *Nucleic Acids Res.*, **44**, 7314–7330.
9. Scott,C.C., Vacca,F. and Gruenberg,J. (2014) Endosome maturation, transport and functions. *Semin. Cell Dev. Biol.*, **31**, 2–10.
10. Im,Y.J., Wollert,T., Boura,E. and Hurley,J.H. (2009) Structure and function of the ESCRT-II-III interface in multivesicular body biogenesis. *Dev. Cell*, **17**, 234–243.
11. Piper,R.C. and Katzmann,D.J. (2007) Biogenesis and function of multivesicular bodies. *Annu. Rev. Cell Dev. Biol.*, **23**, 519–547.
12. Odorizzi,G. (2006) The multiple personalities of Alix. *J. Cell Sci.*, **119**, 3025–3032.
13. Kobayashi,T., Stang,E., Fang,K.S., de Moerloose,P., Parton,R.G. and Gruenberg,J. (1998) A lipid associated with the antiphospholipid syndrome regulates endosome structure and function. *Nature*, **392**, 193–197.
14. Wickner,W. and Schekman,R. (2008) Membrane fusion. *Nat. Struct. Mol. Biol.*, **15**, 658–664.
15. Bissig,C. and Gruenberg,J. (2014) ALIX and the multivesicular endosome: ALIX in Wonderland. *Trends Cell Biol.*, **24**, 19–25.
16. Liang,X.H., Sun,H., Shen,W. and Crooke,S.T. (2015) Identification and characterization of intracellular proteins that bind oligonucleotides with phosphorothioate linkages. *Nucleic Acids Res.*, **43**, 2927–2945.
17. Ceresa,B.P., Lotscher,M. and Schmid,S.L. (2001) Receptor and membrane recycling can occur with unaltered efficiency despite dramatic Rab5(q79l)-induced changes in endosome geometry. *J. Biol. Chem.*, **276**, 9649–9654.
18. Li,G. and Stahl,P.D. (1993) Structure-function relationship of the small GTPase rab5. *J. Biol. Chem.*, **268**, 24475–24480.
19. Ghossoub,R., Lembo,F., Rubio,A., Gaillard,C.B., Bouchet,J., Vitale,N., Slavik,J., Machala,M. and Zimmermann,P. (2014) Syntenin-ALIX exosome biogenesis and budding into multivesicular bodies are controlled by ARF6 and PLD2. *Nat. Commun.*, **5**, 3477.
20. Jefferies,H.B., Cooke,F.T., Jat,P., Boucheron,C., Koizumi,T., Hayakawa,M., Kaizawa,H., Ohishi,T., Workman,P., Waterfield,M.D. *et al.* (2008) A selective PIKfyve inhibitor blocks PtdIns (3,5) P (2) production and disrupts endomembrane transport and retroviral budding. *EMBO Rep.*, **9**, 164–170.
21. Savina,A., Furlan,M., Vidal,M. and Colombo,M.I. (2003) Exosome release is regulated by a calcium-dependent mechanism in K562 cells. *J. Biol. Chem.*, **278**, 20083–20090.
22. Varkouhi,A.K., Scholte,M., Storm,G. and Haisma,H.J. (2011) Endosomal escape pathways for delivery of biologicals. *J. Controlled Release*, **151**, 220–228.
23. Kobayashi,T., Beuchat,M.H., Chevallier,J., Makino,A., Mayran,N., Escola,J.M., Lebrand,C., Cosson,P., Kobayashi,T. and Gruenberg,J. (2002) Separation and characterization of late endosomal membrane domains. *J. Biol. Chem.*, **277**, 32157–32164.
24. Dumas,J.J., Merithew,E., Sudharshan,E., Rajamani,D., Hayes,S., Lawe,D., Corvera,S. and Lambright,D.G. (2001) Multivalent endosome targeting by homodimeric EEA1. *Mol. Cell*, **8**, 947–958.
25. Bissig,C. and Gruenberg,J. (2013) Lipid sorting and multivesicular endosome biogenesis. *Cold Spring Harbor Perspect. Biol.*, **5**, a016816.
26. Pasqual,G., Rojek,J.M., Masin,M., Chatton,J.Y. and Kunz,S. (2011) Old world arenaviruses enter the host cell via the multivesicular body and depend on the endosomal sorting complex required for transport. *PLoS Pathogens*, **7**, e1002232.
27. Sparrow,S.M., Carter,J.M., Ridgway,N.D., Cook,H.W. and Byers,D.M. (1999) U18666A inhibits intracellular cholesterol transport and neurotransmitter release in human neuroblastoma cells. *Neurochem. Res.*, **24**, 69–77.
28. Sobo,K., Le Blanc,I., Luyet,P.P., Fivaz,M., Ferguson,C., Parton,R.G., Gruenberg,J. and van der Goot,F.G. (2007) Late endosomal cholesterol accumulation leads to impaired intra-endosomal trafficking. *PLoS One*, **2**, e851.
29. Liscum,L. (2000) Niemann-Pick type C mutations cause lipid traffic jam. *Traffic*, **1**, 218–225.
30. Lima,W.F., Murray,H.M., Damle,S.S., Hart,C.E., Hung,G., De Hoyos,C.L., Liang,X.H. and Crooke,S.T. (2016) Viable RNaseH1 knockout mice show RNaseH1 is essential for R loop processing, mitochondrial and liver function. *Nucleic Acids Res.*, **44**, 5299–5312.
31. Shen,W., Liang,X.H. and Crooke,S.T. (2014) Phosphorothioate oligonucleotides can displace NEAT1 RNA and form nuclear paraspeckle-like structures. *Nucleic Acids Res.*, **42**, 8648–8662.
32. Liang,X.H., Shen,W., Sun,H., Kinberger,G.A., Prakash,T.P., Nichols,J.G. and Crooke,S.T. (2016) Hsp90 protein interacts with phosphorothioate oligonucleotides containing hydrophobic 2′-modifications and enhances antisense activity. *Nucleic Acids Res.*, **44**, 3892–3907.
33. Shahabipour,F., Barati,N., Johnston,T.P., Derosa,G., Maffioli,P. and Sahebkar,A. (2017) Exosomes: Nanoparticulate tools for RNA interference and drug delivery. *J. Cell. Physiol.*, doi:10.1002/jcp.25766.
34. Alam,M.R., Dixit,V., Kang,H., Li,Z.B., Chen,X., Trejo,J., Fisher,M. and Juliano,R.L. (2008) Intracellular delivery of an anionic antisense oligonucleotide via receptor-mediated endocytosis. *Nucleic Acids Res.*, **36**, 2764–2776.
35. Ming,X., Alam,M.R., Fisher,M., Yan,Y., Chen,X. and Juliano,R.L. (2010) Intracellular delivery of an antisense oligonucleotide via endocytosis of a G protein-coupled receptor. *Nucleic Acids Res.*, **38**, 6567–6576.
36. Miller,C.M., Donner,A.J., Blank,E.E., Egger,A.W., Kellar,B.M., Ostergaard,M.E., Seth,P.P. and Harris,E.N. (2016) Stabilin-1 and Stabilin-2 are specific receptors for the cellular internalization of

phosphorothioate-modified antisense oligonucleotides (ASOs) in the liver. *Nucleic Acids Res.*, **44**, 2782–2794.
37. Crooke,S.T., Wang,S., Vickers,T.A., Shen,W. and Liang,X.H. (2017) Cellular uptake and trafficking of antisense oligonucleotides. *Nat. Biotechnol.*, **35**, 230–237.
38. Wollert,T., Yang,D., Ren,X., Lee,H.H., Im,Y.J. and Hurley,J.H. (2009) The ESCRT machinery at a glance. *J. Cell Sci.*, **122**, 2163–2166.
39. Stuffers,S., Sem Wegner,C., Stenmark,H. and Brech,A. (2009) Multivesicular endosome biogenesis in the absence of ESCRTs. *Traffic*, **10**, 925–937.
40. Martens,S. and McMahon,H.T. (2008) Mechanisms of membrane fusion: disparate players and common principles. *Nat. Rev. Mol. Cell Biol.*, **9**, 543–556.
41. Frolov,V.A., Dunina-Barkovskaya,A.Y., Samsonov,A.V. and Zimmerberg,J. (2003) Membrane permeability changes at early stages of influenza hemagglutinin-mediated fusion. *Biophys. J.*, **85**, 1725–1733.
42. Blumenthal,R., Clague,M.J., Durell,S.R. and Epand,R.M. (2003) Membrane fusion. *Chem. Rev.*, **103**, 53–69.
43. Ming,X., Carver,K., Fisher,M., Noel,R., Cintrat,J.C., Gillet,D., Barbier,J., Cao,C., Bauman,J. and Juliano,R.L. (2013) The small molecule Retro-1 enhances the pharmacological actions of antisense and splice switching oligonucleotides. *Nucleic Acids Res.*, **41**, 3673–3687.
44. Yang,B., Ming,X., Cao,C., Laing,B., Yuan,A., Porter,M.A., Hull-Ryde,E.A., Maddry,J., Suto,M., Janzen,W.P. *et al.* (2015) High-throughput screening identifies small molecules that enhance the pharmacological effects of oligonucleotides. *Nucleic Acids Res.*, **43**, 1987–1996.